(Received 3 October 2023, Accepted 18 January 2024, Scheduled 5 February 2024)

Impact of Laser Cutting on Iron Loss in High Speed Machines

Shruti Singh[1,*], Andrea Credo[2], Ilya Petrov[1], Juha Pyrhönen[1], and Pia Lindh[1]

[1] School of Electrical Engineering, LUT University, Lappeenranta, Finland
[2] University of L'Aquila, Piazzale Ernesto Pontieri, L'Aquila 67100, Italy

ABSTRACT: In electrical machines, most of the iron loss estimation in finite element modeling is based on Bertotti coefficients obtained from the corresponding data sheet. However, often a more exact estimation of coefficients for the laminated steel material is needed. Especially in the case of high speed machines (where iron loss has the highest contribution to the total loss), it is very difficult to estimate the iron loss variation as a result of laser cutting when just using data sheet information as input data in finite element analysis. Laser cutting impacts also the magnetic properties, in terms of magnetization curves at different frequencies, not only the core losses. In this paper, three different core materials of the same lamination steel are prepared to realize the estimation of the Berttotti loss coefficient when the material is subjected to high frequency and under the stress of laser cutting. Experimental analysis is performed to obtain more precise values of Bertotti coefficients at a high frequency range so that they can be utilized in iron loss estimation in a high speed machine (100 krpm maximum speed-1667 Hz) which is further shown as an application. Finally, it is shown how frequency domain iron loss results can be utilized for the time stepping iron loss analysis.

1. INTRODUCTION

Iron losses are in general difficult to evaluate. In addition, manufacturing processes influence the losses and the interaction of physical components, especially when machines are supplied with high frequencies. This effect is relevant also at medium speed when a high number of poles is used (resulting in high electrical frequency). To determine iron loss, most of the methods require the determination of Bertotti coefficients, and the quality of this data determines the accuracy of the iron loss results [1, 2]. Magnetic characteristics deteriorate during machine manufacturing operations such as laser cutting, resulting in higher losses. There are several reasons for the variations in iron loss caused by laser cutting. The heat affected zone is of interest. The laser beam creates heat and exposes the material near the cutting point to very high temperatures. It is easy to understand that heat from the steel's melting point of 1538°C is transferred to some extent to the adjacent material, despite the highly focused laser beam. This heat can cause changes in iron loss characteristics by changing the magnetic properties of the material in the heat-affected region. Rapid temperature changes during laser cutting cause changes in the microstructure of the material. This can affect the magnetic properties of iron [3]. In addition, the laser cutting process can cause a rough cut surface. Changes in surface roughness can alter magnetic flux flow and therefore iron losses. It is vital to note that the magnitude of these modifications will be determined by the laser cutting conditions, the individual material being cut, and the magnetic component's intended application. Researchers and designers working with magnetic components often need to evaluate the effects of manufacturing methods including laser cutting, to ensure that the magnetic circuit parts meet the appropriate requirements.

* Corresponding author: Shruti Singh (shruti.singh@lut.fi).

1.1. Motivation

Because the loss data provided by lamination material producers is based on unprocessed material, it may be not valid for a lamination stack after manufacturing. A designer typically includes additional coefficients in order to simulate these effects. These coefficients depend on the dimensions of the core elements and the manufacturing process. When the share of the core losses of the total losses is high, especially in high frequency machines, the error in the efficiency computation could affect the optimization results. In this case, it is essential to evaluate manufacturing effects in more detail. Material manufacturers data are frequently discovered utilizing established test processes such as Epstein frame test, where a sinusoidally alternating and unidirectional flux magnetizes a flat material sheet. Iron losses are calculated for a given frequency and peak flux density. It is obvious that even a test under this kind of simple setting does not encompass events such as mechanical tensions, microscopic properties, and thermal loads. This raises concerns about the boundaries of material data applicability and if material data can be applied in certain ways that yield more accurate estimates. The frequencies provided by the datasheet providers of laminated steel cannot be commonly used for high frequency applications, i.e., greater than 1 kHz, and they do not include the effect of laser cutting.

1.2. Literature

For an electrical machine consisting of laminated material, mechanical tensions are created when laminations are punched [2]. Shearing stresses affect a number of microscopic processes in the medium [4–6] resulting in a decrease in permeability at the outer edges [7–9]. In addition to the direct effect of the broader hysteresis loop, the tooth center losses are enhanced due to the additional polarization required while edges offer reduced per-

meance and higher flux density, therefore taking place in the middle of the tooth [5]. At higher frequencies, the loss rise at the outer edges is greater [8, 9]. Moreover, the stacked and encapsulation assembly imposes mechanical and thermal loads on the laminated insulation [10]. If the housing is installed with high interference, the surface elements of the steel are subjected to local stresses which reduce the magnetic performance of the machine. These effects are typically neglected in the design steps of the machine.

Loss segregation is a popular technique to calculate losses in rotating equipment, and they are predicted with very simple post processing. Jordan introduced the first loss segregation theory in 1924. It was founded on the notion of splitting losses into static and dynamic parts. The static losses were the hysteresis power loss while the dynamic losses were caused in the lamination due to the rotation assuming that they are distributed homogeneously and are dependent on the electrical conductivity of the material [11]. In [12], Bertotti proposed the extension of this work considering the fact that the eddy current loss distribution is inhomogeneous and dependent on the geometry of the material. Therefore, a third component, anamolous loss was introduced. Bertotti argued that iron losses are so complicated because of the interrelated nature of geometries and material qualities in both time and space that they cannot be accurately predicted. Only statistical data should be used. As a result, dividing the losses among three components allows for the calculation of independent effects on various scales. The Bertotti equation is then given as

$$P_{\mathrm{i,B}} = 1/(\rho)[k_{\mathrm{h}} f B_{\mathrm{m}}^{\alpha} + k_{\mathrm{e}} f^2 B_{\mathrm{m}}^2 + k_{\mathrm{a}} f^{3/2} B_{\mathrm{m}}^{3/2}] \qquad (1)$$

where $P_{\mathrm{i,\,B}}$ is the Bertotti iron loss in W/kg; k_{h}, k_{e}, k_{a} are the hysteresis, eddy current, and anomalous loss constants; f is the operating frequency; ρ is the mass density; B_{m} is the imposed flux density peak value; α varies between 1.6 and 2.2.

1.3. Previous Work

It has been shown in [13] that the actual core flux density is required for the accurate estimation of iron losses in a machine rotating at the speed of 17 krpm. The absolute flux density includes radial flux density, tangential flux density, and harmonics. However, in [14] an Epstein based model is presented where it is shown that Bertotti's equation is applicable to high frequencies up to 2 kHz with alpha equal to 2 when imposed flux densities are kept constant utilizing a two component loss model that includes only hysteresis loss model and an eddy current loss model respectively. In [15], variable coefficients and a look up table loss model are proposed considering a rotational loss factor for the interpolation of iron loss using post processing flux density in the electrical machine. However, different methods proposed in the analysis do not signify an optimum value when being benchmarked against the experimental model. [16] proposes a core loss model where the hysteresis coefficients are variable with frequency and flux density while the eddy currents and anamolous loss coefficients are variable only with the flux density. This phenomenon is only limited to the frequency range of 20–400 Hz. Possible changes in the coefficients due to manufacturing effects are also not indicated. Authors in [17] and [18] have discussed the effect of orthogonal components in flux density due to the rotation of the machine and its effect on the overall losses of the machine. [19] presented an iron loss analysis for a high speed machine considering driving conditions. In this case, the maximum speed goes only till 9 krpm for the high speed machine, and it is shown that when the losses are measured using Epstein frame bench for the frequency range of 100 Hz–1 kHz, the relative error between the experimental values from the machine and the Epstein measured values of the coefficients of iron losses is very low at high flux density. According to the authors' best knowledge, iron loss evaluation for a two-pole 100 krpm machine, where iron loss share is higher than joule loss including the effects of laser cutting, has not been performed yet, and this is the first time that constant values of Bertotti coefficients valid across a broad frequency range (50 Hz–2 kHz) utilizing small frequency increments are provided (using experimentation).

1.4. Contribution

Permeameter measurements are performed to determine the adverse effects of laser cutting in steel laminations. The data is then applied to evaluate the core losses in a 100 krpm machine. The approach uses the segregation of Bertotti coefficients over a large frequency range with small steps of frequency. Also, the electromagnetic stress and iron loss change in the material due to laser cutting at high frequency (i.e., $>$ 1 kHz) are represented. Finally, it is also proposed how frequency domain magnetic characteristics can be utilized in time stepping iron loss analysis.

This paper is divided into four sections. The first section involves the background of various iron loss segregation techniques. The second section consists of an experimental estimation of iron loss coefficients of laser cut lamination sheets over a large frequency range. Small frequency steps are used in the permeameter, and the results are converted into classical Bertotti loss coefficients. This also involves finite element analysis in the frequency domain of the same lamination stack. The third section of the paper involves the validation of the loss coefficients obtained experimentally in the iron loss analysis of the 100 krpm high-speed electrical machine. The losses in this high speed machine are validated using the loss surface method which gives similar results to experimental ones. The fourth section consists of the obtained conclusion.

2. EXPERIMENTAL ANALYSIS

For the experimental analysis, three different types of cores of the same lamination sheet material (M270-35A) are tested using a permeameter. The core materials are processed using a different number of laser cuts as explained below. The experimental model is recomposed in the finite element analysis (FEA) environment for further verification. The properties and setup of the permeameter are also explained in the subsection below.

TABLE 1. Steel materials and parameters utilised in experiment.

Core 1		Core 2				Core 3									
Single laminated ring		Two concentric rings				Five concentric rings									
No cuts		First cut		Second cut		First cut		Second cut		Third cut		Fourth cut		Fifth cut	
ED	ID	ED	ID	ED	ID	ED	ID	ED	ID	ED	ID	ED	ID	ED	ID
60	50	60	55	55	50	60	58	58	56	56	54	54	52	52	50

**ID and ED denote internal and external diameters. All the values are in mm.

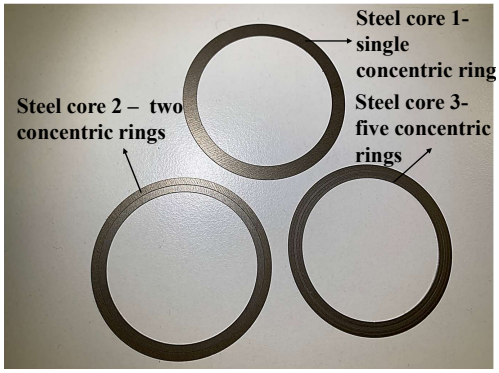

FIGURE 1. Cross section of lamination steel cuts used for testing.

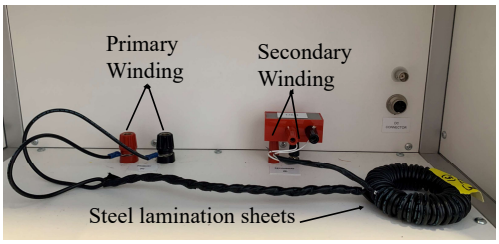

FIGURE 2. Experimental setup of lamination steel sheets and windings inside the permeameter.

2.1. Steel Laminations Selected for the Analysis

Three differently composed steel cores with similar inner and outer diameters are compared in this paper. All the steel core laminations are made of the same material, i.e., M270-35A, and the difference between these three lamination steel cores comes from the laser cuts. Laser cutting is outsourced to a company that manufactures stator and rotor lamination stacks for electric machines. There is no information about the exact characteristics of the laser cutter. Since the company is known for its quality processes, it can be assumed that the procedure is up to date for this application. The first steel core lamination has no internal cuts (only external surfaces were cut by the laser) while the second steel core lamination consists of two concentric rings and has, therefore, four laser cut edges, and the third core lamination consists of five concentric rings having ten laser affected edges altogether as shown in Fig. 1. The parameters of all three steel cores utilized in the experiment are shown in Table 1. The thickness of these lamination sheets is 0.35 mm, and 14 sheets are stacked together to form the laminated stack in the form of toroidal rings.

2.2. Permeameter Setup

For the experimental analysis of the toroidal rings, an AMH-50K-S permeameter by Laboratorio Electrofisico is utilized. The equipment consists of a flux meter, function generator, power amplifier, and digital oscilloscope for the calculation of the above mentioned values at imposed frequencies or flux densities or magnetic fields. The permeameter uses a chamber with terminals for the measurement of the toroidal rings of steel laminations stacked together. There are two couples of terminals inside the chamber. One couple belongs to the measuring winding of the toroid, and the other couple belongs to the excitation winding of the toroid as shown in Fig. 2. The excitation winding is connected to a power amplifier via a shunt resistor while the measuring winding is connected to a digital oscilloscope and a magnetic flux meter. For the analysis of the iron losses, hysteresis curves, and complex permeability of toroidal rings, the power amplifier is made to impose different test frequencies from 50 Hz to 2 kHz. Considering the working rotational speed of the high speed electrical machines, i.e., up to 100 krpm, and for the safe operation of the permeameter for the specific size toroid, a maximum frequency of 2 kHz is taken into consider-

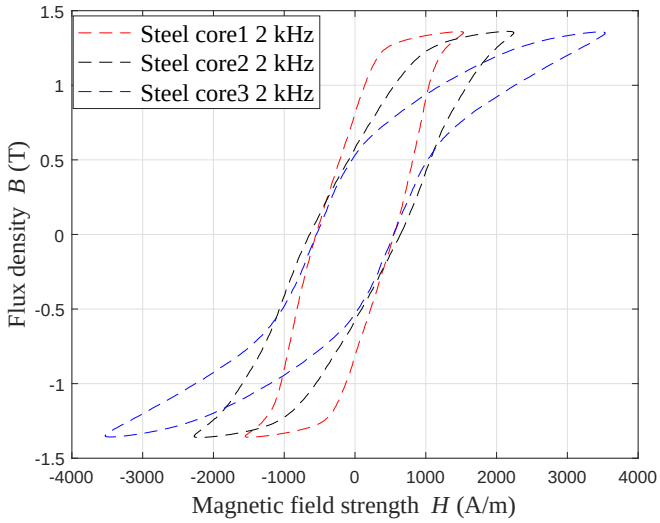

FIGURE 3. Experimental change in hysteresis curves of different steel cores due to different number of laser-cutting-deteriorated areas. The measurement frequency is 2 kHz.

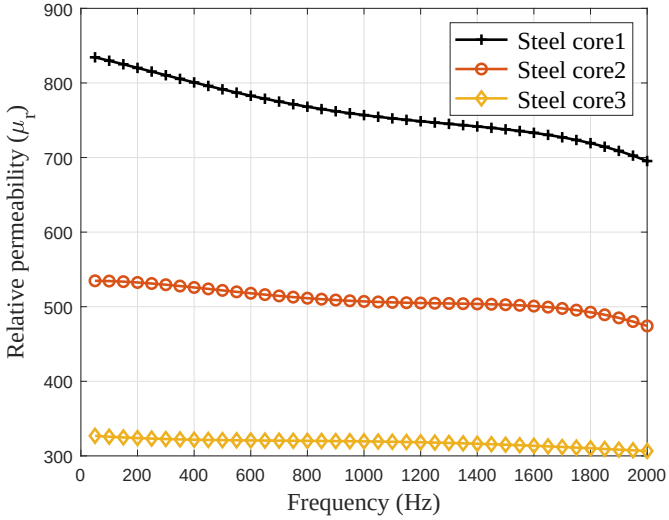

FIGURE 4. Experimental analysis of relative permeability w.r.t. frequency at the imposed flux density of 1.35 T.

ation. To average the data and produce the iron loss and hysteresis curves of the various samples, many tests are conducted at different frequencies. The permeameter results provide the different values of Bertotti coefficients for the analysis of the hysteresis loss, eddy current loss, and extra loss. For the loss model, the permeameter uses the Bertotti equation shown in (1) where the α is automatically set to 2. It is to be noted that the permeameter has a loss error of $\pm 3\%$.

2.3. Effect of Laser Cutting on Permeability

It is indicated in [20] that material permeability after laser cutting is affected mainly by the magnetic field strength H and the sample width. However, they only represent this with the hysteresis curve and power loss distribution. Similarly, [21] shows the effect of laser cutting by indicating the change in flux density from the distance of the cutting edge. [4] presents an analytical 1D dynamic loss model to show the effect of cutting on the local magnetic field induction, but the analytical model does not include the 3D effect. Also, for finite element modeling, a homogenized model is considered to include the cutting effect. In this paper, the change of relative permeability w.r.t. frequency is indicated in all three steel cores to show the effect of laser cutting. Fig. 3 indicates distortion in the hysteresis curve due to a change in permeability. The magnetic field strength H increases with the increase in the number of cuts in the steel core sample. This effect can also be seen through the general relation of relative permeability μ_r with B and H ($\mu_r = B/\mu_0 H$). The relative permeability variation as a function of frequency is shown in Fig. 4. The relative permeability obtained experimentally is fitted through four degrees of the polynomial to show the change of relative permeability w.r.t. frequency. The

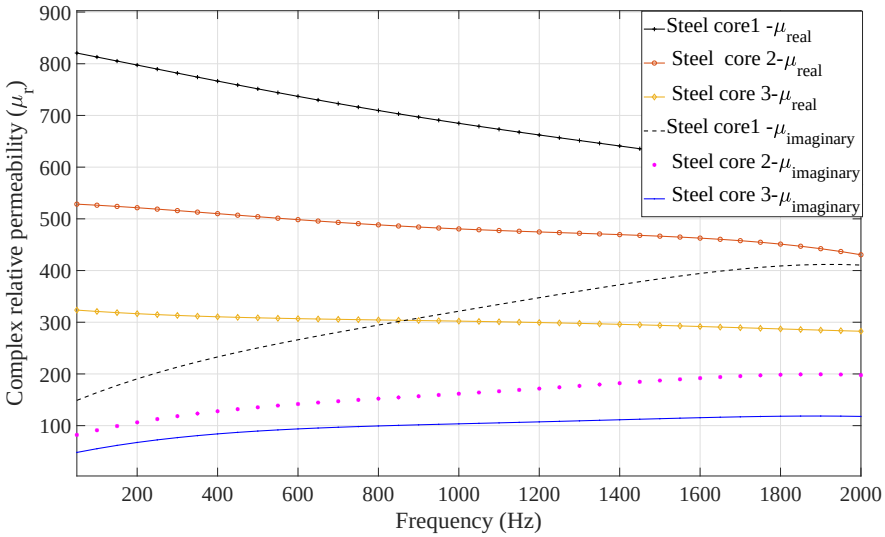

FIGURE 5. Experimentally obtained complex relative permeability variation w.r.t. frequency at the imposed flux density of 1.35 T.

TABLE 2. Step sizes and frequency range for experimentation.

Case	Starting frequency	Final frequency	Frequency step	Number of steps
Case 1	50 Hz	2 kHz	50 Hz	40
Case 2	50 Hz	2 kHz	100 Hz	20
Case 3	50 Hz	1 kHz	50 Hz	20
Case 4	50 Hz	250	50 Hz	5
Case 5	300 Hz	500	50 Hz	5
Case 6	500...:1800 Hz	750...2000 Hz	50 Hz	6 different ranges with 5 steps

relative permeability remains more or less constant as a function of frequency for all the steel laminations. However, due to the presence of laser cut caused defects, a reduction in the relative permeability of the lamination steel can be seen. The major losses at low frequency in lamination steel sheets are hysteresis losses. With the increase in frequency, the loss density increases due to the presence of eddy current losses and anomalous losses. Magnetic flux density and magnetic field strength have a lag because of the inductive nature of the magnetic materials [22]. Although this time lag is minimal at low frequencies at high frequencies, it might be substantial and should be taken into consideration. It is helpful to think of the μ_r as a complex quantity in which real and imaginary parts are functions of f while analyzing the behavior in magnetic cores [23–25].

$$\mu_r = \mu_{re} + i\mu_{im} \tag{2}$$

where μ_{re} and μ_{im} are the real and imaginary parts of the permeability. Fig. 5 represents the fitted experimental values in a four degrees polynomial for the complex permeability in laminated steel and its change with frequency and the impact generated due to the laser cutting. With the increase in frequency, eddy current loss density increases due to an increase in the imaginary part of the complex permeability, and this effect is clearly indicated in [23]. However, in this case, the frequency range is not so high, and still, with the experimental results the effect of the imaginary part of the complex permeability on the eddy current loss density can be seen.

2.4. Estimation of Loss Coefficients Using Permeameter

Steel core 1, steel core 2, and steel core 3 are subjected to the frequencies at a fixed flux density B of 1.35 T and 1.5 T. The reason for choosing this magnetic flux density is that above 1.5 T the current in the excitation winding is very high. Several values of losses are obtained at different frequencies, and fixed B and losses are compared and subjected to interpolation to obtain the values of coefficients of hysteresis k_h, eddy current k_e, and anomalous k_a losses. The permeameter utilizes a fitting algorithm from the total losses, to determine the value of the loss coefficients. To determine the optimal value of the k_h, k_e, and k_a, the iron loss values are measured at different steps of the frequency. The coefficients are computed considering several cases modifying the measurement frequency range and frequency steps according to Table 2. Case 6 represents a multistep analysis varying the starting and the final frequency with a constant frequency step amplitude of 50 Hz.

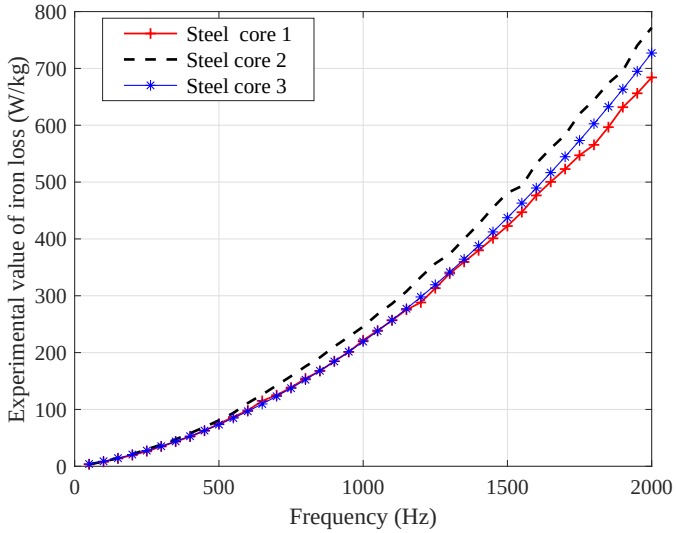

FIGURE 6. Experimental Iron loss analysis for the three cores at different frequencies and the imposed B of 1.35 T.

TABLE 3. Loss coefficients for steel materials (experimentally).

	Core 1			Core 2			Core 3		
Cases	k_h	k_e	k_a	k_h	k_e	k_a	k_h	k_e	k_a
Case 1	278.59	0.551	1.7	305.795	0.553	5.749	304.854	0.6	0.808
Case 2	216.205	0.612	3.197	306.256	0.783	0	490.386	1.032	0
Case 3	279.463	1.170	0	345.913	0.6	2.356	657.166	1.136	0
Case 4	448.759	1.204	0	305.964	1.365	0	795.046	1.250	0
Case 5	629.572	1.193	0	538.032	1.308	0	954.923	1.250	0

*Case 6 is disregarded as it can be seen from Cases 4 and 5 that the coefficients are far away from the actual results.

In the permeameter, the area under the hysteresis curve at different frequencies consists of the total losses of the laminated steel material. Therefore, the area under the hysteresis curve for all three cores is calculated at different frequencies and then compared with the fitting values of the k_h, k_e, and k_a obtained using the fitting algorithm, and the best value of the coefficients is then utilized for the separation of the losses. After the fitting of several cases as shown in Table 2, it is found that when a large number of frequency steps with the widest frequency range is used (50 Hz–2000 Hz presented with case 1), the obtained coefficients have higher accuracy for loss estimation. The maximum values of these losses are obtained at the maximum evaluated frequency. The iron loss densities for steel core 1, steel core 2, and steel core 3 with change in frequency at the imposed B of 1.35 T are indicated in Fig. 6. It can be seen in Fig. 6 that there is not much change in the iron loss density with the number of laser cuts in the lamination material. The loss difference remains negligible at the lower frequencies, but the major variation can be seen in the higher frequency range, i.e., greater than 1 kHz. However, it should be noted that the losses in steel core 3 are lower than in steel core 2. This is because the permeability of the material changes due to laser cutting, but the coercivity remains the same even at high frequency which can be seen in Fig. 3. Therefore, the area under the hysteresis curve does not change at 2 kHz which causes higher losses in core 2 than core 1 and core 3. Moreover, the losses in rings with several cuts are higher than the losses in rings without extra cut. The best fitting coefficients considering the widest frequency range (Case 1) using the permeameter are indicated in Table 3. It can be seen in Table 3 that the indication of anomalous loss changes due to laser cutting is intriguing, and the behavior is not direct. According to [20, 26], laser cutting degrades the material's performance because it modifies the grain size of the electrical steel and therefore the permeability and loss curves. This is a critical aspect of electrical machine design. After all, it is not possible to expect what will be this degradation because it depends on the adopted technology, the speed of the cut, and the size of the cut area. In the design stage of the machine, because the data are not typically available, the designers use coefficients to measure the computed losses. This effect can impact the efficiency of the machine if, in the final application, laser cutting is used for manufacturing; this is typically used for prototyping and small batch production.

2.5. Verification of Loss Coefficients With High Flux Density

To verify the loss coefficients with a higher value of the flux density, the set of coefficients is obtained at $B = 1.35$ T experimentally. Then with this set of coefficients, the iron losses are evaluated at $B = 1.5$ T (black line in Fig. 7, and then these

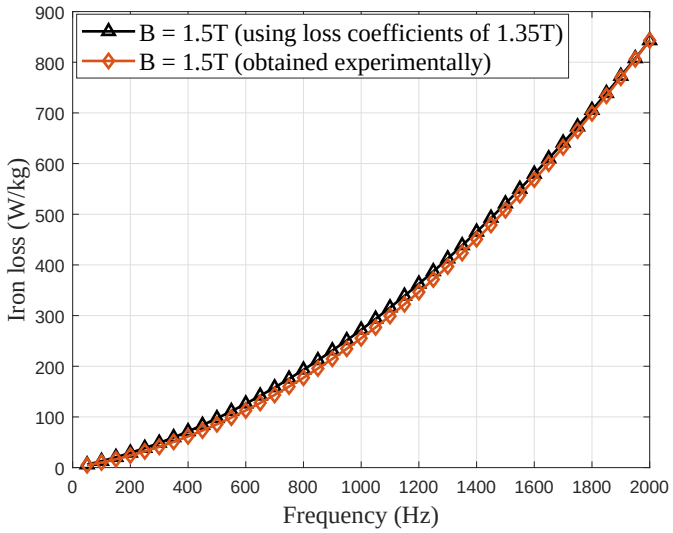

FIGURE 7. Verification of loss coefficients for 1.5 T peak flux density imposed and its comparison with the experimental results at 1.5 T for the steel core 1.

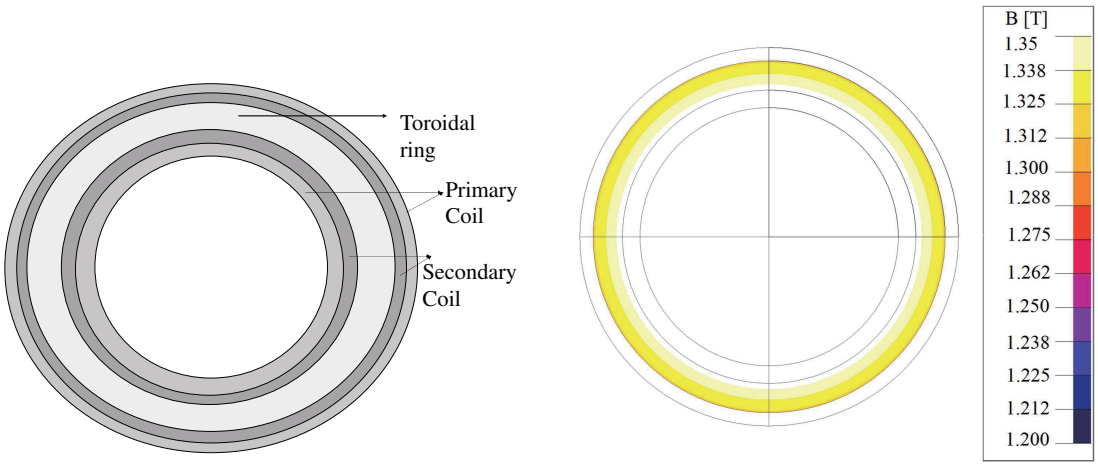

FIGURE 8. (a) Toroidal ring structure. (b) Imposed flux density inside toroidal ring structured for core 1.

losses are compared with the experimental losses at B=1.5 T (orange line in Fig. 7). It can be seen in Fig. 7 that the loss coefficients obtained for 1.35 T work similarly for 1.5 T. Therefore, it is proven that the same loss coefficients work for different flux densities if they are obtained through a large number of steps within a large frequency range. The maximum error is $\leq 6\%$.

2.6. Verification of the Finite Element Model

To verify the finite element model the coefficients obtained by experimental analysis are implemented, and a 2D frequency domain analysis of the toroidal ring without any cuts, i.e., steel core 1 is performed. The reason to choose core 1 is that it has no extra laser cuts and is easy to model in FEA compared to the laser cut models, i.e., core 2 and core 3, respectively. For this analysis, the coefficients and exponents obtained experimentally were utilized. Also, the B-H curve of core 1 and the permeability obtained experimentally using a permeameter are utilized. The toroidal ring in the finite element model consists of a primary coil or excitation winding and a secondary coil, i.e., measuring winding. The excitation coil receives sinusoidal current injection to reach the imposed peak flux density of 1.35 T as the case in experimentation using the permeameter, and a voltage is induced at the secondary coil. The frequency of this current source is varied to obtain losses at different frequencies. The dimensions of the toroidal ring as well as the number of turns in the primary and secondary winding are kept the same as in the experimental analysis. Fig. 8 indicates the excitation and measuring winding regions, the toroidal ring, and the imposed flux density of 1.35 T inside the core.

Figure 9 illustrates that the computed and experimental results match well in the case of steel core 1. The relative difference between the experimental power loss density analysis and the finite element model is $\leq$ 0.5%. Therefore, it can be stated that the finite element model correctly computes the losses when the Bertotti coefficients (obtained within a large

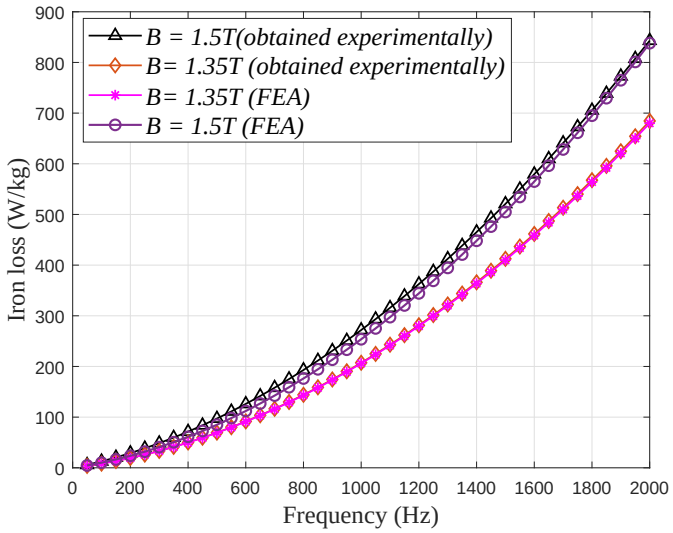

FIGURE 9. Comparison of experimental power loss density with finite element analysis for steel core 1 at 1.35 T and 1.5 T respectively.

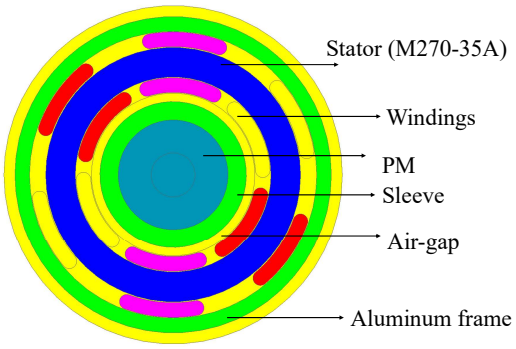

FIGURE 10. Internal structure of the PMSM.

frequency range) are implemented. The analysis above shows good calibration of loss coefficients at different flux densities. In the case of real world applications, the coefficients can be implemented in FEA models to correctly estimate the losses during the design procedures. Knowing the right value of losses allows the designer to optimize the performance according to real data. In the case of electrical machine design, the efficiency is dependent on the losses inside the machine. In case of wrongly estimated losses, the efficiency may be higher or lower depending upon the accuracy of loss coefficients.

3. VALIDATION WITH HIGH SPEED ELECTRICAL MACHINE

Previously in this paper, a frequency domain analysis was performed to determine the loss coefficients and iron losses for the three above mentioned steel cores. To show the impact of laser cutting on the iron losses of a high-speed electrical machine and in order to utilize the magnetic properties obtained through the experimental analysis in the electrical machine, a time-stepping analysis is performed. For this time-stepping analysis, a permanent magnet synchronous machine (PMSM) with a solid rotor is taken into consideration as shown in Fig. 10. The machine parameters are indicated in Table 4. The machine is slotless and provided with a drum winding. The winding consists of Litz wire to reduce the skin effect and proximity effect. The machine is rotating at the speed of 100 krpm and provides a power of 27 kW considering the application for micro-gas turbine. The machine usage and its parameters and basic designing are already explained in [27]. The equivalent air gap of the machine is 16.7 mm. The stator material is NO20; the permanent magnet material is N45UH; and the rotor magnet sleeve is made of Inconel 718 to improve mechanical strength and assembled with a shrink fit to provide optimum fitting at high temperatures and pressure. The stator material is made from M270-35A laminated sheets joined together to form a stack. Fig. 11 shows the magnetic flux density of all the steel cores at the rated values and speed of 100 krpm of the PMSM. The laser cuts are modeled in FEA Altair software by using the different *B-H* curves obtained using experimental analysis with Permeameter.

To see a comparative analysis of the proposed method's accuracy in predicting iron losses compared to conventional methods using standard data sheet information, it is compared with the iron losses obtained by loss-surface (LS) method. LS

TABLE 4. Main parameters of the PMSM.

Parameter	Values
Diameter of permanent magnet	30 mm
External diameter of rotor	38 mm
Active length	100 mm
Number of turns per phase	32
Winding space factor (star connected)	0.5
Number of phases	3
Winding	Distributed
Stator yoke inner diameter	53.4 mm
Stator yoke external diameter	69.6 mm
Rated speed	100000 rpm
Rated frequency	1667 Hz
Number of pole pairs	1
Rated power	27 kW
Rated torque	2.55 Nm
Efficiency expected	95.2%
Rated phase current (RMS)	41 A
Rated phase voltage (RMS)	230 V
Rated current density	18 A/mm^2

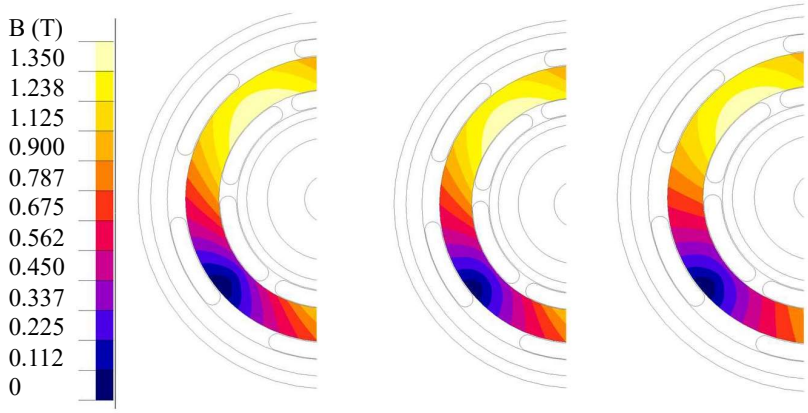

FIGURE 11. Magnetic flux density at the rated load and 100 krpm, Left to right: Steel core 1, Steel core 2, Steel core 3. The laser cuts in the model are simulated using the different *B-H* curves and loss coefficients measured with the permeameter. The difference in magnetic flux density distribution due to laser cutting is hardly visible.

method can be considered as the most reliable among standard iron loss computational methods [28]. The PMSM is subjected to time-stepping analysis at the rated current and the rated speed in Altair Flux. Altair utilizes the model for the iron loss estimation in the materials. The LS model has experimentally determined values of characteristics of the magnetic behavior of the material. This model is explained further in this paper. For this, Altair Flux already has an LS model of the M270-35A. Therefore, to verify the loss model, in the first case, the losses are determined using the LS model in the stator of the machine when working at the rated condition. In the second case, the stator material is replaced with the properties of steel core 1 obtained experimentally, and then the loss coefficients obtained in the above section are utilized in determining the losses.

The relative error in iron loss in PMSM due to changes in coefficients at different step sizes and frequency ranges, compared with the LS method at high speeds, are shown in Fig. 12. It can be stated that the large frequency range with lower step sizes gives closer results to the LS method than the low frequency ranges or fewer step sizes. This comparison aims to demonstrate that it is not possible to correctly estimate the losses if all frequency range is adopted; this could lead to an error in the estimation of losses. The iron loss obtained using the LS method for the M270-35A (stator material) for the above-mentioned PMSM at 100 krpm is 508 W while the iron loss obtained using the properties of core 1 obtained experimentally is 509 W. The difference in the iron loss in both cases is 0.2%. Similarly, the iron losses for core 2 and core 3 are

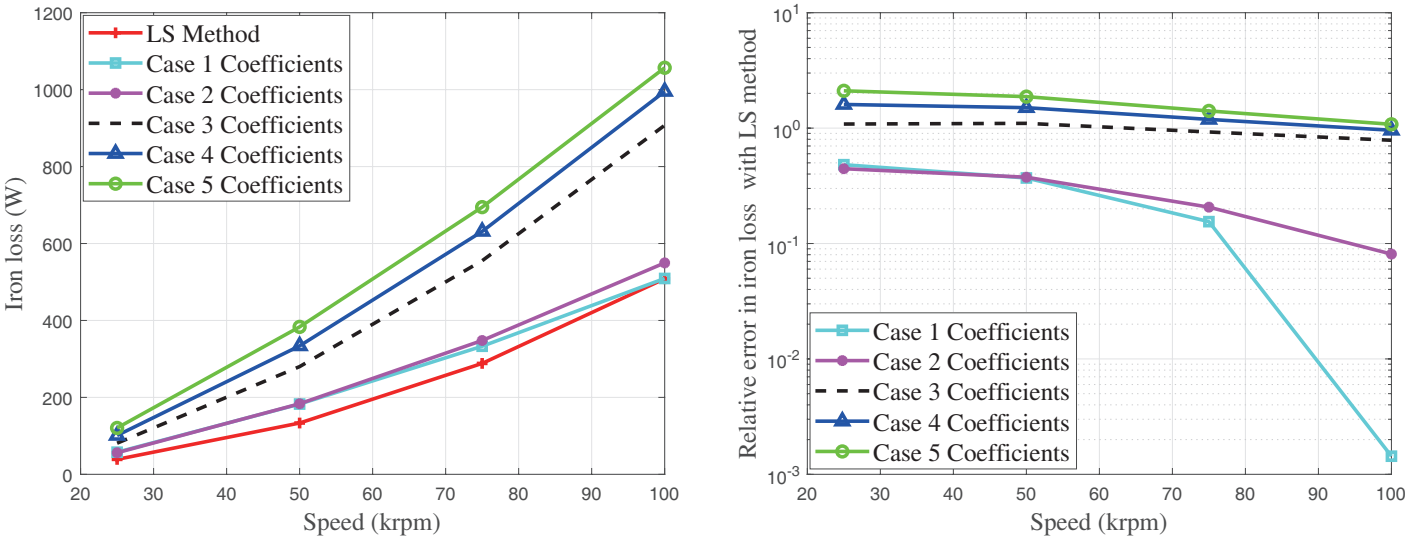

FIGURE 12. Left: Iron loss analysis and Right: Relative loss in iron loss of PMSM at different speeds using coefficients of different cases explained in Tables 1 and 2 respectively. Here the proposed method is compared with the conventional LS method.

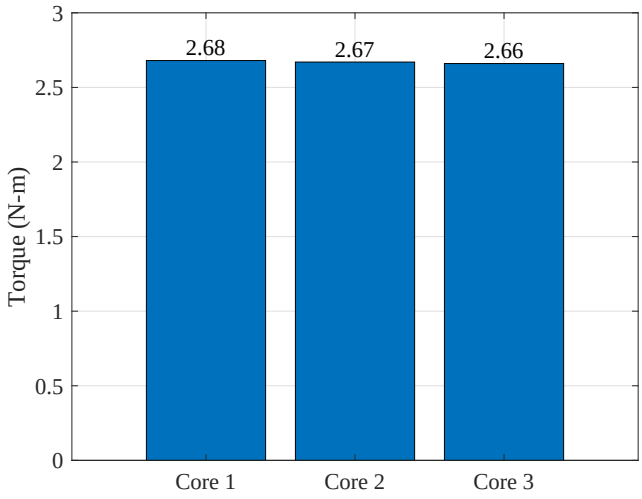

FIGURE 13. Comparison of torque generated by PMSM at the speed of 100 krpm using different core materials obtained using simulations. The laser cuts in the model are simulated using the different *B-H* curves and loss coefficients measured with the permeameter.

579 W and 534 W, respectively. Due to laser cutting the permeability changes which overall changes the torque generated by the machine affecting the overall power generated by the machine. Fig. 13 shows the change in torque due to manufacturing effects using the core materials. In electrical machines having relatively large equivalent air gap (as in the investigated case), the manufacturing effects (e.g. laser cut) have a minor impact on the performance characteristics of the machine. In the case of permeability variation due to laser cutting, some motor types are less sensitive to magnetic circuit permeance fluctuation because of their comparatively wide effective air gap. PMSMs, for example, can have up to ten times the effective air gap of SynRMs (synchronous reluctance machines) or IMs (induction machines). As a result, PMSMs are less affected by iron characteristics mismatch owing to manufacturing impacts. Furthermore, greater power machines may be more resistant to iron characteristics deterioration because of a lower share of excitation current required to the torque generating current than in smaller machines. The manufacturing effect could strongly affect machines with low dimensions because the effects can be strongly pronounced when the total iron area is lower. In addition, especially in the *B-H* curves, the linear part of the curve is strongly affected by laser cut; therefore, the machine designed with PM, which allows working with a minimum level condition in terms of flux density, reduces the effects of the laser cutting. However when, for example, SynRM is designed for low torque (less than 1 Nm) with a reduced dimension of stator tooth and yoke, the laser cutting strongly affects its performance compared to a datasheet material.

3.1. LS Model (Loss-Surface Model)

The LS (Loss Surface) approach is a method for estimating magnetic losses a posteriori that is based on a dynamic hysteresis model coupled with an FEA. The LS model demands that a material's magnetic characteristics are entirely specified, with information regarding its characteristic surface $H(B, \mathrm{d}B/\mathrm{dt})$ (determined empirically). Thus, for a given B(t) signal and frequency, we may ascend via the $H(B, \mathrm{d}B/\mathrm{dt})$ surface to the H(t) field and reconstruct the appropriate dynamic cycle of hysteresis. The characteristic surface $H(B, \mathrm{d}B/\mathrm{dt})$ of each material can be obtained using a medium frequency Epstein frame bench for magnetic measurements. An analytical model allows the reconstruction of the H field from B values:

$$H\left(B, \frac{\mathrm{d}B}{\mathrm{d}t}\right) = H\mathrm{static}(B) + H\mathrm{dynamic}\left(B, \frac{\mathrm{d}B}{\mathrm{d}t}\right) \quad (3)$$

While any static model may be used to model the static part, the dynamic part is modeled using the LS model. The parameter Hdynamic(B, dB/dt) is calculated completely through experimentation, using evaluations on an Epstein frame, then recorded in a reference table, allowing Hdynamic to be reconstructed at all magnetic states within the measurement range using linear interpolation, simple computational representation, or polynomial curve fitting. As a result, the three components (B, dB/dt, Hdynamic) generate a single characteristic surface Hdynamic as a function of (B, dB/dt). B(H) curves can therefore be produced, allowing for very precise calculations of iron losses. It involves FEA utilizing the Altair Flux program to obtain the B(t) forms of every component and apply the model to calculate the local and global losses. It is already shown in [28] that the difference between experimental iron loss and iron loss calculated using LS method for high speed machines (up to 50 krpm) is about 14%. Similarly, the dependence of the LS method on the frequency is explained in [29].

4. CONCLUSION

The following conclusion is obtained from this paper:

- The Bertotti loss coefficients utilizing (1) can be used for the iron loss estimation if a small frequency step amplitude with a large number of frequency steps is used in measurements. This was verified experimentally. In the case of real world applications, the coefficients can be implemented in FEA models to correctly estimate the losses during the design.
- The loss coefficients show good calibration when different flux densities are imposed (experimentally and using FEA).
- Experimentally, the losses in core 2 are higher than in core 1 and core 3. This shows that the laser cut changes the permeability of the material, but the coercivity remains the same at higher frequencies ($\geq$ 600 Hz) which is visible from the hysteresis curve shown in the paper at 2 kHz.
- Behaviour of anomalous loss in steel material changes when the laser cut effect is introduced and still needs to be studied in future works. One possible direction of further research is to apply microscopic analysis of the cut edge surface after different laser cut techniques (by varying temperature/power and timing of the laser cut) and measure iron loss in each case.
- Complex permeability and its dependence on laser cutting and iron loss variation are indicated.
- Loss coefficients obtained using (1) by frequency domain analysis over a large number of steps for a large frequency range are utilized in the time-stepping iron loss analysis of the high-speed PMSM. The iron losses are then compared with the iron losses obtained experimentally using the LS method for the same machine using the same materials. The dependence of torque on the permeability of the material is also indicated.
- It can be concluded that compared to low frequency ranges or fewer step sizes, the widest frequency range with smaller step sizes produces results that are closer to the LS approach. The analogy tries to illustrate that when all frequency range is used, it is impossible to estimate losses appropriately, which might result in an inaccuracy in loss estimates.

ACKNOWLEDGMENTS

This project has received funding from the Ministry of Culture and Education, Finland, and was conducted with the support of the Academy of Finland's Centre of Excellence in High-Speed Energy Conversion Systems.

REFERENCES

[1] Hargreaves, P. A., B. C. Mecrow, and R. Hall, "Calculation of iron loss in electrical generators using finite-element analysis," *IEEE Transactions on Industry Applications*, Vol. 48, No. 5, 1460–1466, 2012.

[2] Krings, A., "Iron losses in electrical machines-influence of material properties, manufacturing processes, and inverter operation," Ph.D. dissertation, Ph.D. dissertation, KTH Royal Institute of Technology, 2014.

[3] Abo-Seida, O. M., N. T. M. El-dabe, A. R. Ali, and G. A. Shalaby, "Cherenkov FEL reaction with plasma-filled cylindrical waveguide in fractional D-dimensional space," *IEEE Transactions on Plasma Science*, Vol. 49, No. 7, 2070–2079, Jul. 2021.

[4] Hofmann, M., H. Naumoski, U. Herr, and H.-G. Herzog, "Magnetic properties of electrical steel sheets in respect of cutting: Micromagnetic analysis and macromagnetic modeling," *IEEE Transactions on Magnetics*, Vol. 52, No. 2, 2000114, Feb. 2016.

[5] Vandenbossche, L., S. Jacobs, F. Henrotte, and K. Hameyer, "Impact of cut edges on magnetization curves and iron losses in e-machines for automotive traction," *World Electric Vehicle Journal*, Vol. 4, No. 3, 587–596, 2010.

[6] El-Dabe, N. T. M., A. R. Ali, A. A. El-shekhipy, and G. Shalaby, "Non-linear heat and mass transfer of second grade fluid flow with hall currents and thermophoresis effects," *Appl. Math.*, Vol. 11, No. 1, 267–280, 2017.

[7] Moses, A. J., N. Derebasi, G. Loisos, and A. Schoppa, "Aspects of the cut-edge effect stress on the power loss and flux density

distribution in electrical steel sheets," *Journal of Magnetism and Magnetic Materials*, Vol. 215, 690–692, Jun. 2000.

[8] Saleem, A., N. Alatawneh, R. R. Chromik, and D. A. Lowther, "Effect of shear cutting on microstructure and magnetic properties of non-oriented electrical steel," *IEEE Transactions on Magnetics*, Vol. 52, No. 5, 2001904, May 2016.

[9] Al-Timimy, A., G. Vakil, M. Degano, P. Giangrande, C. Gerada, and M. Galea, "Considerations on the effects that core material machining has on an electrical machine's performance," *IEEE Transactions on Energy Conversion*, Vol. 33, No. 3, 1154–1163, 2018.

[10] Boubaker, N., D. Matt, P. Enrici, F. Nierlich, and G. Durand, "Measurements of iron loss in PMSM stator cores based on CoFe and SiFe lamination sheets and stemmed from different manufacturing processes," *IEEE Transactions on Magnetics*, Vol. 55, No. 1, 1–9, 2018.

[11] Jordan, H., "The ferromagnetic constants for weak alternating fields," *Elec. After. Techn.*, Vol. 1, No. 8, 1924.

[12] Bertotti, G., *Hysteresis in Magnetism: For Physicists, Materials Scientists, and Engineers*, Gulf Professional Publishing, 1998.

[13] Zhang, Y., S. McLoone, and W. Cao, "Electromagnetic loss modeling and demagnetization analysis for high speed permanent magnet machine," *IEEE Transactions on Magnetics*, Vol. 54, No. 3, 8200405, 2017.

[14] Ionel, D. M., M. Popescu, M. I. McGilp, T. J. E. Miller, S. J. Dellinger, and R. J. Heideman, "Computation of core losses in electrical machines using improved models for laminated steel," *IEEE Transactions on Industry Applications*, Vol. 43, No. 6, 1554–1564, 2007.

[15] Leandro, M., N. Elloumi, A. Tessarolo, and J. K. Nøland, "Analytical iron loss evaluation in the stator yoke of slotless surface-mounted PM machines," *IEEE Transactions on Industry Applications*, Vol. 58, No. 4, 4602–4613, 2022.

[16] Ionel, D. M., M. Popescu, S. J. Dellinger, T. J. E. Miller, R. J. Heideman, and M. I. McGilp, "On the variation with flux and frequency of the core loss coefficients in electrical machines," *IEEE Transactions on Industry Applications*, Vol. 42, No. 3, 658–667, 2006.

[17] Hernandez-Aramburo, C. A., T. C. Green, and A. C. Smith, "Estimating rotational iron losses in an induction machine," *IEEE Transactions on Magnetics*, Vol. 39, No. 6, 3527–3533, Nov. 2003.

[18] Stranges, N. and R. D. Findlay, "Measurement of rotational iron losses in electrical sheet," *IEEE Transactions on Magnetics*, Vol. 36, No. 5, 3457–3459, 2000.

[19] Seo, J.-H., T.-K. Chung, C.-G. Lee, S.-Y. Jung, and H.-K. Jung, "Harmonic iron loss analysis of electrical machines for high-speed operation considering driving condition," *IEEE Transactions on Magnetics*, Vol. 45, No. 10, 4656–4659, 2009.

[20] Sundaria, R., D. G. Nair, A. Lehikoinen, A. Arkkio, and A. Belahcen, "Effect of laser cutting on core losses in electrical machines — Measurements and modeling," *IEEE Transactions on Industrial Electronics*, Vol. 67, No. 9, 7354–7363, 2019.

[21] Siebert, R., J. Schneider, and E. Beyer, "Laser cutting and mechanical cutting of electrical steels and its effect on the magnetic properties," *IEEE Transactions on Magnetics*, Vol. 50, No. 4, 2001904, 2014.

[22] Boutabba, N., "Nonmagnetic negative refractive index media based on chalcogenide glasses," *Appl. Math.*, Vol. 17, No. 2, 223–226, 2023.

[23] Abeywickrama, K. G. N. B., T. Daszczynski, Y. V. Serdyuk, and S. M. Gubanski, "Determination of complex permeability of silicon steel for use in high-frequency modeling of power transformers," *IEEE Transactions on Magnetics*, Vol. 44, No. 4, 438–444, Apr. 2008.

[24] Islam, S., B. Halder, and A. R. Ali, "Optical and rogue type electrical soliton solutions of the (2+1) dimensional nonlinear heisenberg ferromagnetic spin chains equation," *Scientific Reports*, Vol. 13, 9906, 2023.

[25] Osman, M. S., K. U. Tariq, A. Bekir, A. Elmoasry, N. S. Elazab, M. Younis, and M. Abdel-Aty, "Investigation of soliton solutions with different wave structures to the (2+1)-dimensional heisenberg ferromagnetic spin chain equation," *Communications in Theoretical Physics*, Vol. 72, No. 3, 035002, 2020.

[26] Manescu, V., G. Paltanea, H. Gavrila, and I. Peter, "The influence of punching and laser cutting technologies on the magnetic properties of non-oriented silicon iron steels," in *2014 International Symposium on Fundamentals of Electrical Engineering (ISFEE)*, Bucharest, Romania, Nov. 2014.

[27] Singh, S., I. Petrov, J. Pyrhönen, and P. Sergeant, "Conceptual design of high-speed permanent-magnet generator for a micro gas turbine," in *2022 International Conference on Electrical Machines (ICEM)*, Valencia, Spain, 2022.

[28] Vo, A.-T., M. Fassenet, V. Preault, C. Espanet, and A. Kedous-Lebouc, "New formulation of loss-surface model for accurate iron loss modeling at extreme flux density and flux variation: Experimental analysis and test on a high-speed pmsm," *Journal of Magnetism and Magnetic Materials*, Vol. 563, 169935, 2022.

[29] Zhu, Q., Q. Wu, W. Li, M.-T. Pham, and L. Zhu, "A general and accurate iron loss calculation method considering harmonics based on loss surface hysteresis model and finite-element method," *IEEE Transactions on Industry Applications*, Vol. 57, No. 1, 374–381, 2021.